79-7045

INITIAL WIND TUNNEL TESTS AT MACH 4 AND 7 OF A HYDROGEN-BURNING, AIRFRAME-INTEGRATED SCRAMJET

Robert W. Guy* and Ernest A. Mackley**
NASA Langley Research Center
Hampton, Virginia

Abstract

A research investigation of a new, fixed-geometry, hydrogen-burning scramjet engine concept, designed for total airframe integration, is currently in progress at NASA's Langley Research Center. Two heavily instrumented engine models incorporate inlet and combustor designs developed previously in component tests. Initial tests of these subscale engine models are being conducted in ground facilities at conditions simulating flight at Mach numbers 4 and 7. The scramjet test results which are presented include inlet performance, ignition/reaction aids, inlet-combustor interactions, and engine performance in terms of thrust balance measurements and internal pressure and heating rate distributions. The relationship of these results to flight engine performance is discussed.

Nomenclature

A_c	geometric capture area (normal to airstream), 0.033 m^2
$C_{\Delta F}$	$\frac{\Delta F}{q_\infty A_c}$, force coefficient based on force balance ΔF
C_T	$\frac{\text{Thrust}}{q_\infty A_c}$, net installed thrust coefficient
h	inlet height (fig. 10), cm
L_I	ignition delay length, cm
M	Mach number
p	static pressure, kN/m^2
P_t	airstream stagnation pressure, MN/m^2
q	airstream dynamic pressure, kN/m^2
$\dot{q}$	wall heating rate, MW/m^2
T	static temperature, K
T_t	airstream stagnation temperature, K
x	distance from scramjet sidewall leading edge (fig. 10), cm
y	distance from scramjet top surface (fig. 10), cm
ΔF	difference in measured force between fuel on and fuel off, N
ϕ	fuel equivalence ratio - ratio of fuel flow rate to stoichiometric flow rate
η_c	combustion efficiency

Subscripts

adjusted	adjusted to account for unburned fuel
corr	corrected to T_t = 890K and q_∞ = 47.88 kN/m^2
inj	injected
N	injected normal to airstream at struts
reac	reacted or burned
t	total
1	upstream of inlet
∞	upstream of aircraft bow shock

*Aerospace Engineer, Hypersonic Propulsion Branch, High-Speed Aerodynamics Division
**Aerospace Engineer, Hypersonic Propulsion Branch, High-Speed Aerodynamics Division. Member AIAA

Introduction

At Mach numbers above 6, engine cycle studies have shown that the hydrogen-burning supersonic combustion ramjet (scramjet) has unique performance advantages over other airbreathing engines.[1] In particular, the airframe-integrated scramjet now undergoing extensive research at NASA's Langley Research Center has the potential for high thrust and efficiency with low drag, weight, and cooling requirements.[2,3]

In the airframe-integrated approach, several scramjet modules would be placed side-by-side on the airframe undersurface such that the vehicle forebody provides a compression surface for the engine airflow and the vehicle aft section provides part of the nozzle expansion surface (fig. 1). The side-by-side grouping of the modules provides an engine inlet capable of capturing a large portion of the flow compressed by the aircraft bow shock. Another advantage of the modular arrangement is that a single module is of a size and shape more suited to testing in ground facilities.

The fixed-geometry inlet of the scramjet has 48° swept surfaces and a cutback cowl (fig. 2) which permits increased flow spillage and inlet starting at low flight Mach numbers. Inlet compression is provided by the sidewalls in the horizontal direction as opposed to that provided by the aircraft forebody in the vertical direction. The inlet compression process is completed by three 48° swept struts (fig. 2) which results in a shorter inlet. Previous inlet component tests[4], in conventional ground facilities at simulated flight Mach numbers from 3 to 7, have demonstrated performance rivaling variable geometry inlets (fig. 3).

The three swept struts are also used for multiplane, instream fuel injection which permits a shorter combustor because of faster fuel-air mixing.[2] Extensive direct-connect tests of the scramjet fuel injector-combustor concept have been performed[5-7] and tests continue in an effort to refine the concept. Combustor heat release is controlled by modulation of perpendicular and parallel fuel injection from the struts.[8] At high flight Mach numbers ($M_\infty > 7$), most of the fuel would be injected normal to the airstream to achieve rapid mixing and burning; however, at lower Mach numbers ($M_\infty < 5$), most of the fuel would be injected parallel to the airstream to prevent excessively rapid mixing and burning which could thermally choke the engine.

The major portion of the scramjet nozzle is a half nozzle formed by the aircraft aft end (fig. 1). Calculations indicate that the nozzle area ratio provided by the aircraft increases thrust significantly.[2] The nozzle flow is supersonic throughout and is complicated by nonuniform entrance flow, by multi-component reacting species, by internal shock and viscous effects, by interactions at the nozzle exit between adjacent module wakes, and by interactions with flow spilled from the engine inlet.

The nozzle is being studied analytically[9] and experimental tests include simulation of the nozzle flow with gases other than air.[10]

Using results from the component tests and from theoretical guidelines, two hydrogen-burning, component-integration models of the airframe-integrated scramjet have been designed and fabricated. These models include the complete module inlet and combustor but only the initial part of the nozzle, i.e., nozzle exit area is approximately equal to the inlet area.

The purpose of the engine model test program is to perform research on the airframe-integrated scramjet concept as opposed to demonstration tests of a developed engine. This research is underway with tests of the inlet-combustor module in ground facilities at simulated flight Mach numbers of 4 and 7. These test Mach numbers were chosen because they provide data representative of engine operation over a broader Mach number range. For instance, at Mach 4, most of the fuel is injected parallel to the airflow, but at Mach 7 (and above) most of the fuel is injected perpendicular to the airflow. In addition, at Mach 4, inlet spillage is large (≈ 34%) while at Mach 7, inlet spillage is small (≈ 6%).

Several problems related to facility limitations may be anticipated in these tests which would not necessarily be experienced in flight. For instance, facility power requirements (especially at Mach 7) limit both the scale of the model that can be tested and the flight altitude that can be simulated. These limitations can lead to ignition and reaction problems because of short residence times in subscale models and long ignition and reaction times at high simulated altitudes.

The possibility of interaction problems between the inlet and combustor may also be anticipated when these two components are integrated for the first time. The engine model tests will provide information to guide further component tests to improve inlet and combustor design. The test program is planned to continue through several engine generations as component interactions are eliminated and the inlet, combustor, and fuel injector concepts are refined to optimize scramjet performance.

This paper is a status report on the research investigation of the airframe-integrated scramjet. After a description of the scramjet models and the test facilities, the test program is discussed from its inception including inlet performance, techniques to enhance ignition and reaction, inlet-combustor interactions, and scramjet performance for various fuel equivalence ratios.

Apparatus

Models

Two scramjet engine models have been used in the Mach 4 and 7 tests. Both have rectangular frontal areas 20.32 cm high by 16.26 cm wide and their lengths are 142.2 cm and 151.1 cm, respectively. The engine which has been tested at simulated Mach 7 flight conditions is constructed of copper and is primarily heat-sink cooled with water cooling only in high heat flux areas such as leading edges.[11] The engine which has been tested at simulated Mach 4 flight conditions is constructed from Nickel 200 and is a heat-sink engine with no active cooling. Both engines are heavily instrumented to measure internal wall static pressures, temperatures, and heating rates (copper engine only). External instrumentation consists of pressures measured on forward-facing surfaces and on the base of the engine. In addition, both models are mounted in the test facilities on one-component force balances to measure thrust and drag. A photograph of the copper engine with the external cover plates removed, exposing the instrumentation leads and cooling lines, is shown in figure 4 and the nickel engine is shown in figure 5.

Both engines are designed as research models to allow substitution of components which vary in internal shape. For instance, the inlet, combustor, nozzle, and fuel injection struts can each be replaced without affecting the other components. Thus, the models can serve as test beds for various component designs without having to build a completely new model.

The inlet designs of the two engines are quite similar except that the nickel engine employs a "drooped" internal cowl surface to relieve the amount of local flow compression in the cowl region. This is most important at Mach numbers below 5. Internal area distributions aft of the inlet are somewhat different with the nickel engine incorporating an updated combustor design. A comparison of the internal geometries of the two engines is shown in figure 6. The combustor expansion begins earlier in the nickel engine with less expansion occurring on the sidewalls and less compression on the top surface.

Test Facilities

The facilities used for Mach 4 and 7 scramjet tests are shown in the photographs in figures 7 and 8, respectively, and a schematic of the Mach 7 test arrangement is shown in figure 9 (Mach 4 arrangement is similar). The Mach 4 facility is located at the General Applied Science Laboratories (GASL) in Westbury, N.Y., and the Mach 7 Scramjet Test Facility is located at NASA's Langley Research Center. Both facilities incorporate several features essential to airframe-integrated scramjet tests.

First, the enthalpy levels of Mach 4 (T_t = 890K) and Mach 7 (T_t = 2220K) flight are duplicated in the facilities. This is accomplished in the Mach 4 facility by hydrogen-air combustion with oxygen replenishment to replace that used in heating the test stream. Therefore, the test stream contains water vapor as well as nitrogen and oxygen. As will be explained later, the Mach 4 facility was operated at total enthalpies above the Mach 4 enthalpy level for some of the tests reported here. Mach 7 enthalpy is achieved by heating the air with a 10 megawatt d.c. electric arc.

Second, the facilities simulate the bow shock precompression that would occur in flight prior to the air entering the engine. The forebody precompression is simulated by expanding the Mach 4 and 7 energy flows to only 3.4 and 6, respectively, at the exits of the facility contoured nozzles. However, the engine nozzle expansion area provided by the aft section of the aircraft, which accounts for 30 to 50 percent of the net thrust, is not simulated in the tests.

Third, the models can be mounted in the facility test sections so that a portion of the facility nozzle top surface boundary layer is ingested by the scramjet (fig. 9). This partially simulates the ingestion of the aircraft undersurface boundary layer by a flight engine.

Fourth, the installed thrust/drag of the scramjet engine models is measured by the force balances. The measured drag is actually somewhat high relative to that expected in flight since only one module is involved and drag from two external sidewalls is included. In flight, a grouping of several modules would only have two external sidewalls.

The Mach 4 facility stagnation pressure ranged from 0.38 MN/m^2 to 0.70 MN/m^2. This simulated flight altitudes from 21,000 to 25,000 m, i.e., flight dynamic pressures from 52.7 to 28.5 kN/m^2 which covers the engine design flight dynamic pressure, 47.9 kN/m^2. The Mach 7 facility stagnation pressure was 3.04 MN/m^2. Due to present facility power limitations, the engine tests simulated only 40 percent (19.2 kN/m^2 or 35,350 m altitude) of the engine design flight dynamic pressure. A more detailed description of the Mach 7 facility can be found in reference 12.

Mach 7 Scramjet Tests

Ninety tests have been conducted on the scramjet in the Mach 7 facility between April 1977 and February 1979. Early tests without fuel injection were used to verify that the inlet started and that performance was the same as in previous component tests.[13] The verification is shown in figure 10 by the excellent agreement between data from the engine tests and data from the inlet component tests. Data are in close agreement with theoretical estimates[13] of inlet pressures except near the cowl where a shock is generated by downflow from the swept inlet shocks.

Early in the test series, a facility-model interaction was observed. During this interaction, which was caused by combustion of the hydrogen fuel, the test cabin pressure around the model increased. This generated shock waves from the facility nozzle which impinged on forward-facing surfaces of the engine, causing increased drag and, at high fuel flows, often resulted in inlet unstarts. This problem was solved by facility and test procedure modifications.

The remainder of the tests have been concerned with techniques to achieve ignition and sustain reaction, to eliminate inlet-combustor interactions, and to increase engine performance. In the Mach 7 tests reported here, only hydrogen fuel injection from the struts perpendicular to the airflow was employed. Fuel temperature varied from 430-640K (as a function of fuel flow rate) due to aerodynamic heating of the struts.

Ignition/Reaction Aids

Difficulty in achieving ignition and sustaining reaction was encountered immediately in the Mach 7 tests. As mentioned in the Introduction, factors contributing to ignition delay are the small engine scale and low combustor entrance pressure level due to higher altitude flight simulation than that for which the engine was designed (at combustor entrance: $p \approx 29.2$ kN/m^2; $T \approx 860$K). Internal engine geometry can also be a factor by failing to maintain pressure levels high enough to sustain reaction. Low fuel temperature and low engine wall temperatures also act to aggravate ignition and reaction problems in the heat-sink engine relative to a regeneratively cooled flight engine.

Several simple techniques were employed in an attempt to achieve ignition and sustain reaction. These techniques are not necessarily suitable for a flight engine, but were used in the research model simply as quick and easy means to ignite and burn the fuel so that the test program could proceed to explore other potential problem areas in the airframe-integrated scramjet concept.

One ignition technique involved adding attachments to the center strut aft end to decrease flow expansions just downstream of fuel injection and thereby increase static pressure and temperature in this region. These attachments also increased the scale of the strut base region. Two such attachments were used and are labeled "center strut modifications 1 and 2" in figure 11. In conjunction with this ignition technique, a method designed to sustain reaction in the combustor consisted of injecting a small quantity of air or nitrogen (about 7.5% of the air captured by the inlet) about one-third of the combustor length downstream from the entrance (fig. 11). The gas was injected in an upstream direction from orifices in tubes located on both sidewalls. The idea was to use the gas injection to decrease the 12.4° sidewall expansion in this region, i.e., the technique simulated a geometry change in the combustor. With this ignition/reaction enhancement scheme, the first evidence of heat release in the combustor varied in location as a function of the amount of fuel injected.

Ignition was also achieved by adding zirconium oxide rods to center strut modification 1 to act as ignitor/flameholders (fig. 12). These rods protruded approximately one-third of the distance to the side strut. Movies confirmed ignition in the region of the rods. With this ignitor, reaction was sustained by a combustor geometry modification. Sidewall plates were added internally in the combustor to create a constant area section 15.2 cm long at the combustor entrance as shown in figure 12. This constant area section decreased flow expansions just downstream of the struts and maintained a higher pressure level to avoid quenching the reaction.

Because of the ignition problems, component research is now underway to explore different and more useful ignition aids. Also, additional Mach 7 tests at pressures up to two and one-half times those of the present tests will be underway shortly. These test conditions will approximate the design flight dynamic pressure of the engine and ignition/reaction problems should be greatly diminished.

Inlet-Combustor Interactions

Burning in the scramjet was often accompanied by varying degrees of inlet-combustor interaction ranging from an increase in inlet pressures near the cowl (with some increased flow spillage) to complete inlet unstarts. The onset of interaction was a function of combustor geometry, the amount of fuel burned, and the amount of facility nozzle top

surface boundary layer ingested by the engine.

To reduce the amount of boundary layer ingested, the model was dropped 2.54 cm into the flow. This change reduced the interaction problem and a higher fuel equivalence ratio could be injected and burned before interaction occurred. A force balance data trace showing such a test with fuel equivalence ratios of 0.5 and 1.0 is shown in figure 13. Local interaction occurred near the cowl at both fuel equivalence ratios. Stoichiometric fuel injection was achieved for a short period of time (approximately 1/2 sec.) but with increased flow spillage in the cowl region and with eventual inlet unstart (probably associated with increasing wall temperature with time). Note that the total drag of the module is just overcome with stoichiometric fuel injection; however, the fuel-off drag was high because of the zirconium oxide rod ignitors used and because of high external drag with the engine dropped into the flow (part of the external top surface was contributing to the drag).

With the geometry modifications required for ignition, the inlet-combustor interaction problem persists at reacted fuel equivalence ratios above approximately 0.3. Several approaches are being evaluated to control this adverse inlet-combustor interaction. They include inlet-combustor isolation steps, fuel injector modifications, and various splits between perpendicular and parallel fuel injection.

Tests of the inlet are also underway in a conventional wind tunnel where combustion is simulated by air injection to further define the cause of the inlet-combustor interaction and to find a solution. It should be noted that the ignition/reaction and inlet-combustor interaction problems are not necessarily independent problems in that the changes necessary for ignition and reaction at low pressure may make the inlet more sensitive to combustor pressure rise.

Engine Performance

Typical internal sidewall pressure and heat transfer rate distributions with and without hydrogen combustion are shown in figure 14. Center strut modification 2 was used to achieve ignition and nitrogen injection was used to sustain the burning. The pressure data, obtained near the engine midheight line with stoichiometric fuel injection, show little effect of combustion upstream of the fuel injection line (data nearer the cowl do show an upstream effect). The large increases in pressures and heating rates in the combustor are evidence of hydrogen combustion.

Engine performance from these initial tests is shown in figure 15 as a function of the injected fuel equivalence ratio. The figure of merit for engine performance used here is ΔF, i.e., the force balance measurement with fuel injection minus the force balance measurement with no fuel injection. ΔF indicates internal performance, but gives no indication of the magnitude of internal drag. The one-dimensional theory curve shown on the figure represents the maximum expected performance for the engine with ignitors and modified combustor geometry and with all perpendicular fuel injection, mixing-controlled reaction and 100 percent combustion efficiency. Open symbols are data obtained using the strut aft end modifications to achieve ignition and the nitrogen injection technique to sustain reaction; shaded symbols are data obtained using zirconium-oxide rods as ignitor/flameholders and the combustor geometry change to sustain reaction.

Dashed line fairings have been placed through the open-symbol data where strut modifications and the nitrogen injection technique were used to aid ignition and sustain reaction. The right-hand single point (with dashed line) is data taken with no strut modification. The next dashed line fairs data taken using modification 1 to the center strut aft end to eliminate expansions upstream of the base. The upper dashed line fairs data taken with modification 2 (fig. 11) which is designed to further increase compression after fuel injection. The higher compression apparently causes earlier ignition and, consequently, higher combustion efficiency. The data indicate that the highest performance in terms of increased ΔF is obtained with strut modification 2 and the nitrogen injection technique or with the zirconium-oxide rods and the combustor sidewall modification. Near $\phi_{inj} = 0.5$, the fuel injection struts coated with zirconium oxide (to increase surface temperature) appear to enhance burning relative to the uncoated struts. However, performance is still well below the theoretical estimates for complete combustion, and at the higher fuel flows, data with significant burning (upper dashed curve) are obtained with some increased inlet spillage (as indicated by increased pressures on the external cowl surface).

The difference between the data and theory is likely due to the combined effects of low combustion efficiency, inlet-combustor interaction, and long ignition delay. In an effort to resolve these differences, estimates of combustion efficiency, η_c, were made for the data in figure 15 with the exception of that obtained with the zirconium rods and the combustor geometry modification. This modification eliminated some heat flux measurements essential to a determination of combustion efficiency. The estimates of η_c were obtained from an engine performance computer program which integrates heating rates in the combustor and calculates combustion efficiency from a correlation by Orth, Billig, and Grenleski.[14]

When the data from figure 15 are replotted with ΔF as a function of the estimated reacted fuel equivalence ratio, i.e., $\phi_{reac} = \eta_c \phi_{inj}$, the data correlation is quite good (fig. 16). However, at the lower values of ϕ_{reac}, the measured ΔF's are significantly below theory. Inspection of internal heating rate distributions (fig. 17) indicated that one reason for this could be longer ignition delay lengths, L_I, at the lower fuel equivalence ratios. Therefore, theoretical estimates were made of the expected ΔF using the following assumptions: fuel-air mixing corresponding to perpendicular fuel injection,[8] combustion efficiency as determined from measured heating rates,[14] and ignition point as indicated by the location where the measured wall heating rate shows an increase above the value with no fuel injection as shown in figure 17. The results of the theoretical estimates are shown by the dashed line in figure 16. The trend of the theoretical estimate is very similar to that of the data lending support to the hypothesis that the poor performance at low ϕ_{reac} could be caused by ignition delay.

It is also noted in figure 16 that the estimated ϕ_{reac} does not exceed 0.5. Although some spillage was occurring at this level of reacted fuel equivalence ratio (with a possible effect on the estimated combustion efficiency), the implication is that only about one-half of stoichiometric burning has been achieved. Research is underway to define the cause of this problem since the airframe-integrated scramjet must operate at reacted fuel equivalence ratios near one in flight.

Therefore, the challenge in the airframe-integrated scramjet research program is to achieve ignition and obtain higher combustion efficiency without inlet-component interaction at fuel flow rates near stoichiometric values. It is also necessary to have a configuration that is compatible with engine operation at lower Mach numbers.

Mach 4 Scramjet Tests

Near Mach 4 the present scramjet concept was expected to be more susceptible to inlet-combustor interaction problems. The inlet sweep (48°), combined with the inlet Mach number of 3.4 (which simulates the flow field on the underside of the vehicle forebody), results in detached shock waves around the inlet struts. Because of the associated relatively low Mach number at the inlet throat, inlet interaction resulting from the combustor pressure rise was expected. Also, one-dimensional theoretical calculations indicated the probability of thermal choking in the combustor downstream of the struts for supersonic combustion at levels of ϕ_{reac} above about 0.4 to 0.6. Raising the total temperature in these calculations above Mach 4 simulation (890K) raises the ϕ level at which thermal choking occurs.

For the above reasons, the Mach 4 test condition was selected as a particularly important one in the present research program. Over seventy tests at Mach 4 have been made during 1978. The inlet wall static pressure distributions with both cold and hot tunnel flow at about the same Reynolds number were first checked with those from reference 4 to verify proper operation of the inlet. In the first series of tests, a facility-model (combustion) interaction was experienced which was similar to the interaction encountered in the Mach 7 tests, but it was eliminated by installation of a tunnel diffuser.[15] The sensitivity of the inlet to combustor pressure rise (inlet-combustor interaction) was expected to be worse with the top wall tunnel boundary layer entering the scramjet model. The Mach 7 tests had already yielded results indicating that this was true.

The remainder of the tests have been concerned with techniques to eliminate inlet-combustor interaction and to increase engine performance. The hydrogen fuel injection was split between the perpendicular and parallel modes with a maximum of 25% of the total being injected perpendicular to the airflow. Hydrogen entered the fuel injection struts at ambient temperature.

Ignition Aid

At Mach 4 enthalpy level, the air static temperature ($T \approx 550K$, $p \approx 101\ kN/m^2$) in the scramjet at the point of fuel injection is not high enough for autoignition to occur within a reasonable length. Therefore, an ignitor will be required for flight application and an effort is underway to develop such an ignitor. For the preliminary ground tests, it was decided to use a surge in the stream total temperature during the initial part of the test to provide ignition.

In order to achieve a high stream total temperature (1390K) at the beginning of a test for hydrogen ignition and a lower stream total temperature for the test condition, extra hydrogen is initially added in the facility heater (along with normal air, H_2, and O_2 flow rates). After the scramjet ignition is established, the extra hydrogen flow is cut off and the lower stream total temperature of the test condition is established along with the proper O_2 simulation of air. Additional reduction in total temperature has been achieved by simply increasing the heater air flow rate above the initial set condition.

The use of initially high stream total temperature, followed by a reduction in this temperature to achieve a steady-state run condition involves transients in stream total pressure, air flow rate, and fuel equivalence ratio. A typical variation with time of measured engine force, fuel equivalence ratio, and stream total temperature and pressure is shown in figure 18. The engine fuel was brought to a constant level of mass flow and held steady. The indicated changes in equivalence ratio occur because of the changes in air flow rate (caused by the changes in stream total pressure and temperature). The desired steady-state test condition was achieved in the latter part of the test.

Inlet-Combustor Interaction

As expected, and as experienced at Mach 7, inlet-combustion interaction occurred during the early Mach 4 testing. Lowering the scramjet engine model 2.54 cm down into the flow resulted in less inlet-combustor interaction problems and permitted an increase in fuel equivalence ratio before interaction occurred. In general the occurrence of interaction was worse for equivalence ratios greater than 0.5, but as predicted, increased stream total temperatures resulted in less interaction. As shown in figure 18, interaction often occurred when the stream total temperature was being reduced from the ignition level to the nominal run condition.

Efforts were made to resolve the interaction in the strut region by moving the fuel injection away from the top, cowl, and sidewalls and by installing rearward facing steps in the walls ahead of the normal fuel injection station. These efforts seemed to have had small favorable effects but did not eliminate the interaction problem.

The Mach 4 scramjet engine model is currently being altered for future tests. Fuel will be injected from the walls at a station near the downstream end of the combustor to avoid thermal choking at high fuel equivalence ratios. The engine would then operate in a mixed combustion mode where part of the fuel would be burned supersonically in the first part of the combustor and the remainder of the fuel would be burned subsonically further downstream. This dual mode combustion should allow achievement of high performance at Mach numbers less than about 5.

Engine Performance

Most of the tests conducted to date in the Mach 4 test series have been at stream total temperatures above the Mach 4 flight simulation value. In order to show a comparison with theory and to present all the data at the same test conditions, the force data (ΔF is the change in measured force from fuel on to fuel off) was corrected to the Mach 4 total temperature, 890K, and a dynamic pressure of 47.88 kN/m^2. The correction for dynamic pressure, which assumes that the thrust coefficient at a given fuel equivalence ratio is constant over the range of pressures tested, was made by using the ratio of the nominal stream total pressure (0.634 MN for q_∞ = 47.88 kN/m^2) to the actual stream total pressure. A correction also was made for stream total temperature by multiplying ΔF_{meas} by the square root of the ratio of the measured stream total temperature to the nominal M = 4 stream total temperature (890K). This assumes that the specific impulse is constant and necessarily is a more arbitrary correction than the correction for dynamic pressure.

The corrected force data are plotted as a function of injected fuel equivalence ratio in figure 19 and are compared with theoretical performance predictions for η_C = 100 percent at the nominal test condition (M_∞ = 4, q_∞ = 47.88 kN/m^2, T_t = 890K). For the curve shown, it was assumed that a fuel equivalence ratio, ϕ_N, of 0.05 was injected normal to the flow at the struts and the remainder was injected from the rear of the struts parallel to the flow. Although increasing the percentage of fuel injected normal to the flow at the struts up to ϕ_N of about 0.2 increases the thrust (ΔF) for ϕ_t values up to about 0.5, almost no difference is noted above ϕ_t = 0.5 where the mixed combustion mode (partial burning supersonically, remainder subsonically) is used for the theoretical calculations. To simplify this presentation only the predicted ΔF values for ϕ_N = 0.05 are shown, but the thermal choking limits in ϕ_t are shown for both ϕ_N = 0.05 and ϕ_N = 0.195. The Mach 4 experimental data indicate a limit in ϕ_t which strongly suggests thermal choking, but it is noted that this occurred at generally higher stream total temperatures than the nominal Mach 4 value (890K) used for the theory. A few data points agree very well with predictions at ϕ_{inj} levels up to 0.4. Another obvious factor is that there is a second group of data which can be represented by a line faired parallel to the theoretical curve. A review of the fuel injection schedule indicated that for nearly all of the higher equivalence ratio data, the extra fuel was injected parallel to the test stream from the rear of the side struts. It is possible that the side strut fuel is not igniting until further downstream when the combustion in the center of the stream mixes out to reach the side strut fuel (and air). Making the arbitrary assumption that only a part of this parallel fuel from the side struts burned, one data point was selected and a factor found which would move the data point to the theoretical curve. This adjustment factor assumes only one-third of the side strut parallel fuel burns but also simultaneously would assume 100 percent combustion for all other fuel.

Using this assumed factor, all of the data were adjusted and replotted as shown on figure 20, but the change in force, ΔF_{corr}, is now plotted as a function of adjusted equivalence ratio similar to the ϕ reacted data shown for Mach 7. Figure 20 shows that the data now are in good agreement with the theoretical prediction. The exact value of the adjustment factor is not important to the conclusion that the parallel fuel from the side struts is not burning completely. Review of the adjustment of other data points further supports the above conclusion, but the reason for the incomplete combustion is not yet obvious from the data analysis. However, it is concluded that the engine has performed well in some tests, that the remaining problems are defined, and that with further research, the desired performance will be achieved at Mach 4.

Relationship Between Subscale and Flight Engine Performance

Tests of single, subscale modules of the airframe-integrated scramjet can only partially simulate the installed performance that would be expected in flight. A single module has two external sidewalls which create drag while a group of several modules in the flight case would have only two external sidewalls. Therefore, the flight engine external drag would be less. An even greater effect is the larger nozzle area of the flight engines. The subscale model has a nozzle exit area equal to geometric capture area while a flight engine, with the aircraft aft end as part of the nozzle, would have a nozzle exit-to-inlet capture ratio on the order of 3.5. Therefore, a projection of the test results to a flight application is considered informative and is shown in figures 21 and 22.

For the test results, the most readily determined and accurate performance parameter is ΔF, i.e., the change in measured engine force with and without fuel injection. Using this force change in coefficient terms, $C_{\Delta F}$, predictions were made for fuel equivalence ratios of 0.4 and 1.0 (with 100 percent combustion efficiency) using a one-dimensional theory[16] which accounts for forebody precompression, internal heat losses, and a nozzle exit-to-capture area ratio of one. With ϕ = 1.0, the theory indicates that a mixed mode of combustion (supersonic-subsonic) is required to avoid thermal choking for Mach numbers below 5. Therefore, the ϕ = 1.0 curve assumes a dual mode of combustion for low Mach numbers. For ϕ = 0.4, the mode of combustion is supersonic over the entire Mach number range.

It is important to note the limitations of the one-dimensional theoretical predictions in defining the scramjet internal performance. The application of experimentally determined heat release data is less certain because of small differences in internal geometry and scale, changes in combustion mode, fuel temperature, wall temperature, etc. Based on a relatively large number of calculations, the uncertainty in the one-dimensional theory values of performance shown in this paper is about plus or minus 10 percent.

In figure 21, experimental data obtained at Mach 4 and 7 (Mach 4 data corrected for stream total temperature) with ϕ_{inj} = 0.4 are compared with the one-dimensional theory. Data agreement with theory at ϕ_{inj} = 0.4 is quite good at Mach 4 which implies near 100 percent combustion efficiency. At Mach 7, and ϕ_{inj} = 0.4, the comparison with theory reflects the lower combustion efficiency discussed earlier in the paper. This is further emphasized by the second data point at Mach 7 with

ϕ_{reac} = 0.4 (combustion efficiency derived experimentally) which is in good agreement with the theory. The ϕ = 1.0 theoretical curve for ground tests shown in figure 21 remains as the goal to be reached in terms of ΔF.

For ground tests, one-dimensional theoretical predictions of the scramjet internal performance can be made by using the best available input to allow for the mixing, ignition heat release, and heat balance effects.[16] Engine interactions, such as thermal choking, can also be anticipated. In relating the theoretical prediction at ϕ = 1.0 for ground tests (fig. 21) to flight engine net installed thrust performance (fig. 22), proper accounting must be made for an installation of about six flight engines with appropriate internal and external drag, heat transfer differences (regenerative cooling for flight), forebody angle relative to the flight path, forebody boundary layer, and larger flight engine nozzle areas (nozzle exit-to-inlet capture area ratio of 3.5 compared to a ratio of 1 for the ground tests). The curve in figure 22 represents the predicted flight performance for the installed scramjet at ϕ = 1.0. Below Mach 5, it is assumed that a mixed mode of combustion will be required with only a relatively small amount of fuel burned subsonically at Mach 5 and on the order of ϕ = 0.6 burned subsonically at Mach 4. With the level of installed flight performance indicated in figure 22, it has been shown in reference 17 that an aircraft can be designed with an integrated scramjet to cruise efficiently at hypersonic speeds.

Concluding Remarks

A preliminary airframe-integrated scramjet research program was conducted at test conditions simulating Mach 4 and 7 flight. These conditions were selected because of the differences in the way the hydrogen fuel is injected and in the differences in air flow captured. Problems of ignition and inlet-combustor interaction were predicted which needed experimental definition. A prime research objective of the Mach 4 and 7 tests was to achieve the highest possible conbustion efficiency by varying the fuel injection scheme and by modifying the engine internal geometry.

Considerable progress has been made in understanding and solving the predicted ignition/reaction and inlet-combustor interaction problems. Simple techniques for achieving ignition during the ground test programs at both Mach 4 and 7 were shown to be feasible. Incomplete reaction of the fuel at Mach 4 has been traced to the poor combustion of fuel injected parallel to the flow from the side struts. At Mach 7, the ignition/reaction problems can be associated with the present high altitude simulation of the facility. The inlet-combustor interaction problems at both Mach numbers were shown to be partially the result of tunnel top wall boundary layer ingestion, which is necessary for proper simulation of the airframe-integrated concept. When the scramjet models were positioned outside the tunnel boundary layer, a larger fuel equivalence ratio could be reached before inlet-combustor interaction occurred. At Mach 4, thermal choking of the combustor was evident (for $\phi_{reac} > 0.4$ to 0.6) as a second type of inlet-combustor interaction. Stoichiometric burning at this Mach number will require either a combustor geometry change or injection of a portion of the fuel in the downstream end of the combustor.

The research program has defined the problems which were predicted by analysis. Since most of these problems are interactive, their resolution is not direct. Separate programs have been initiated or are continuing in ignitor/ignition research, inlet-combustor interaction research, and scramjet configuration-related supersonic combustor research. Secondly, the Mach 4 and 7 scramjet test programs are continuing with revised fuel injection schemes, geometric changes, and more favorable test conditions (at Mach 7). Beyond this, research plans call for revised engine designs and further testing.

Within the limitations of facilities and the scramjet models used in the preliminary tests, scramjet engine performance data have been obtained whtich agree well with theoretical predictions at reacted fuel equivalence ratios up to 0.5. With this as a beginning, it is expected that the predicted performance can be achieved at higher fuel equivalence ratios, when the problems described above are resolved. With this accomplished, the fixed-geometry, airframe-integrated scramjet will provide efficient airbreathing propulsion at Mach numbers above 4.

Acknowledgments

This paper presents data from the first tests of component integration models of the Langley airframe-integrated scramjet concept and represents results of a group research effort. Personnel of the Hypersonic Propulsion Branch at Langley Research Center contributed to obtaining and analyzing the Mach 4 and 7 data. Personnel of the General Applied Science Laboratories, Inc. obtained and assisted in analyzing the Mach 4 data.

References

[1]Waltrup, Paul J.; Anderson, Griffin Y.; and Stull, Frank D.: "Supersonic Combustion Ramjet (Scramjet) Engine Development in the United States," presented at the 3rd International Symposium on Airbreathing Engines, Munich, Germany, March 1976.

[2]Henry, J. R.; and Anderson, G. Y.: "Design Considerations for the Airframe-Integrated Scramjet," presented at the 1st International Symposium on Airbreathing Engines, Marseille, France, June 19-23, 1972.

[3]Jones, Robert A.; and Huber, Paul W.: "Airframe-Integrated Propulsion System for Hypersonic Cruise Vehicles," presented at the 11th Congress of the International Council fo the Aeronautical Sciences, Lisbon, Portugal, Sept. 10-16, 1978.

[4]Trexler, Carl A.: "Inlet Performance of the Integrated Langley Scramjet Module," presented at the AIAA/SAE 11th Propulsion Conference, Anaheim, California, Sept. 29 - Oct. 1, 1975, AIAA preprint No. 75-1212, Sept.1975.

[5]Anderson, Griffin Y.; Reagon, Patricia G.; Gooderum, Paul B.; and Russin, W. Roger: "Experimental Investigation of a Swept-Strut Fuel-Injector Concept for Scramjet Application," NASA TN D-8454, Aug. 1977.

[6]McClinton, Charles, R.; and Gooderum, Paul B.: "Direct-Connect Test of a Hydrogen-Fueled, Three-Strut Injector for an Integrated Modular Scramjet Engine," presented at the Fourteenth JANNAF Combustion Meeting, Colorado Springs, Colorado, Aug. 15-17, 1977.

[7]McClinton, Charles, R.: "Interaction between Step Fuel Injectors on Opposite Walls in a Supersonic Combustor Model," NASA Technical Paper 1174, May 1978.

[8]Anderson, Griffin Y.: "An Examination of Injector/Combustor Design Effects on Scramjet Performance," presented at the 2nd International Symposium on Airbreathing Engines, Sheffield, England, Mar. 25-29, 1974.

[9]Dash, S. M.; and Del Guidice, P. D.: "Numerical Methods for the Calculation of Three-Dimensional Nozzle Exhaust Flow Fields," NASA SP-347, Part I, Mar. 1972.

[10]Hunt, J. L.; Talcott, N. A., Jr.; and Cubbage, J. M.: "Scramjet Exhaust Simulation for Hypersonic Aircraft Nozzle Design and Aero Model Tests, presented at the AIAA 15th Aerospace Sciences Meeting, Los Angeles, California, Jan. 24-26, 1977, AIAA preprint No. 77-82, Jan. 1977.

[11]Guy, Robert W.; Mueller, James N.; Pinckney, Shimer Z.; and Lee, Louise P., "Thermal Design and Analysis of a Hydrogen-Burning Wind Tunnel Model of an Airframe-Integrated Scramjet," NASA TM X-73931, Jan. 1977.

[12]Boatright, William B.; Sabol, Alexander P.; Sebacher, Daniel I.; Pinckney, Shimer Z.; and Guy, Robert W.: "Langley Facility for Tests at Mach 7 of Subscale, Hydrogen-Burning, Airframe-Integratable Scramjet Models,: presented at the AIAA 14th Aerospace Sciences Meeting, Washington, D. C., Jan. 26-28, 1976.

[13]Trexler, Carl A.; and Souders, Sue W.: "Design and Performance at a Local Mach Number of 6 of an Inlet for an Integrated Scramjet Concept," NASA TN D-7944, Aug. 1975.

[14]Orth, R. C.; Billig, F. S.; and Grenleski, S. E.: "Measurement Techniques for Supersonic Combustion Testing," AIAA Progress in Astronautics and Aeronautics, Vol. 34, Jan. 1974.

[15]Andrews, Earl H., Jr.: "Design and Subscale Tests of a Diffuser System for a Mach 4 Scramjet Test Facility," presented at the AIAA 10th Aerodynamic Testing Conference, San Diego, California, April 19-21, 1978. AIAA Paper No. 78-771, Apr. 1978.

[16]Pinckney, S. Z.: "Internal Performance Predictions for Langley Scramjet Engine Module," NASA TM X-74038, Jan. 1978.

[17]Weidner, J. P.; Small, W. J.; and Penland, J. A.: "Scramjet Integration on Hypersonic Airplane Concepts," presented at the AIAA/SAE 12th Propulsion Conference, Palo Alto, California, July 26-28, 1976.

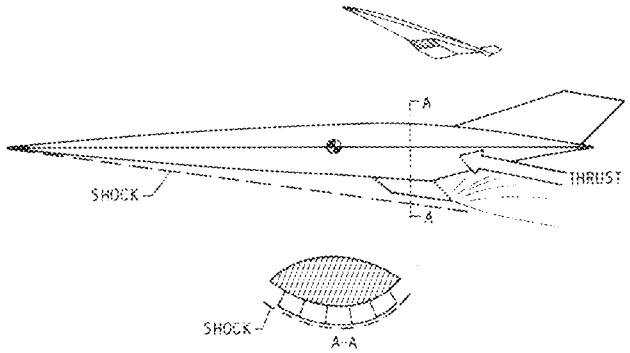

Fig. 1 Scramjet-vehicle integration.

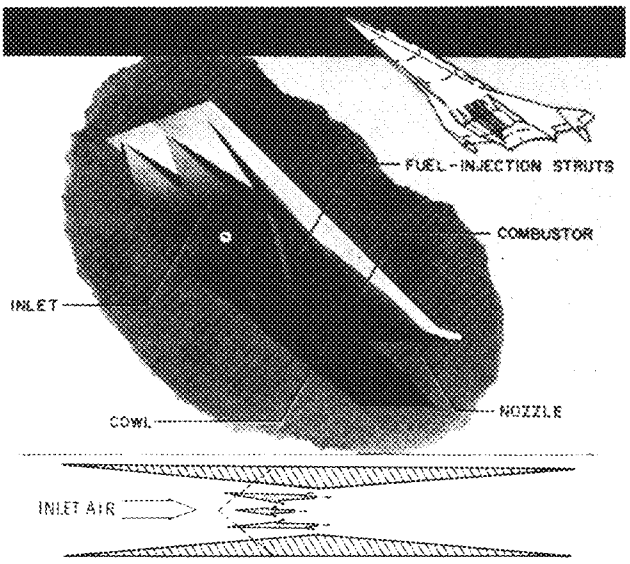

Fig. 2 Airframe-integrated supersonic combustion ramjet.

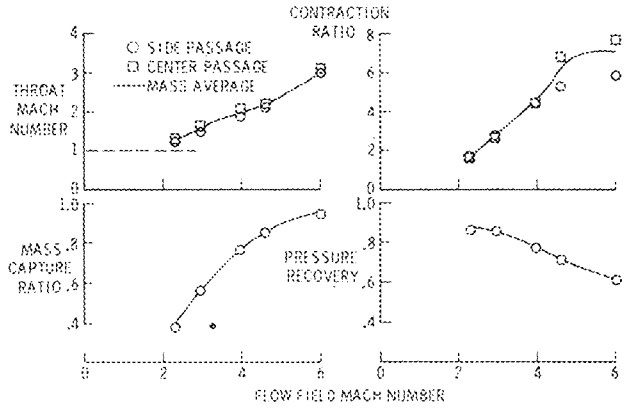

Fig. 3 Scramjet module inlet performance.

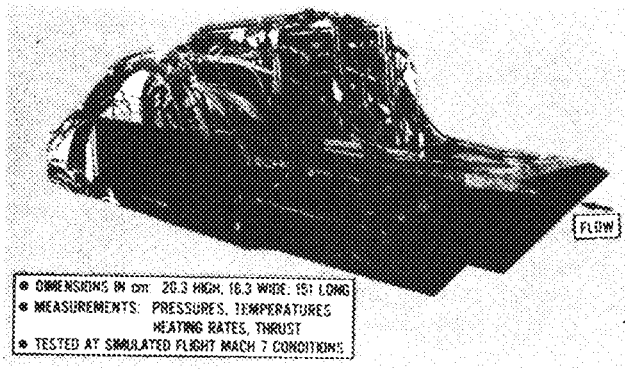

Fig. 4 Copper scramjet engine model.

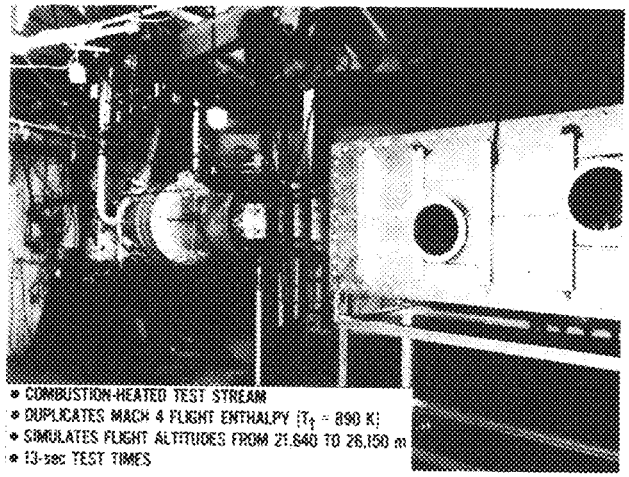

Fig. 7 Mach 4 scramjet test facility at GASL.

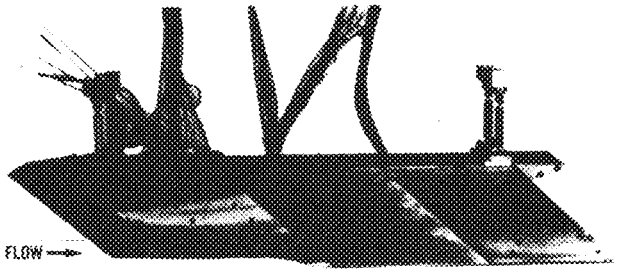

Fig. 5 Nickel scramjet engine model.

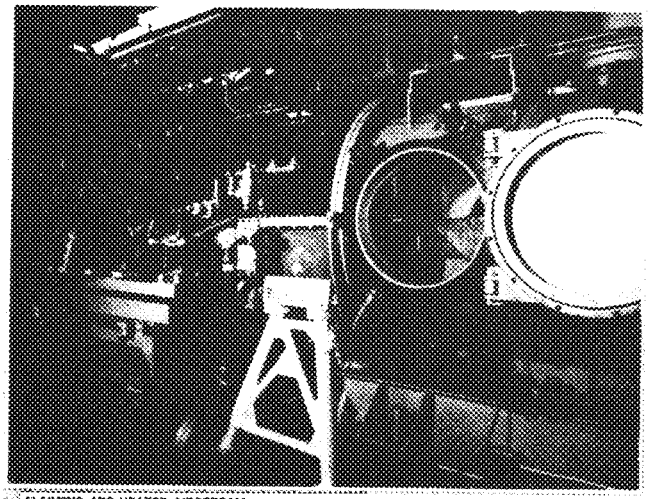

Fig. 8 Mach 7 scramjet test facility.

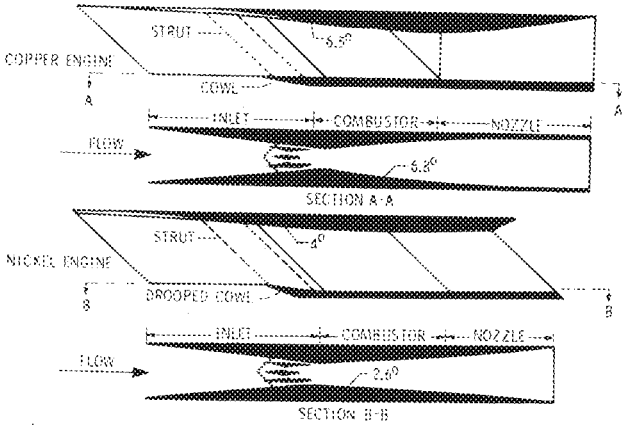

Fig. 6 Model internal contour comparison.

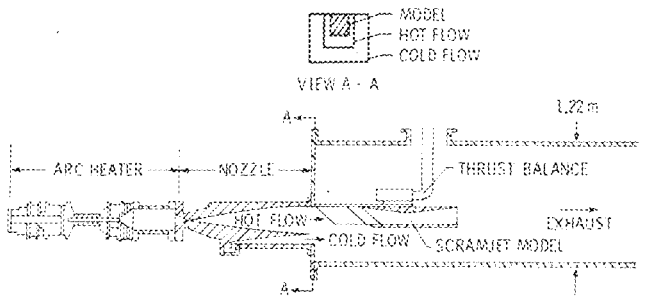

Fig. 9 Test arrangement in Mach 7 facility.

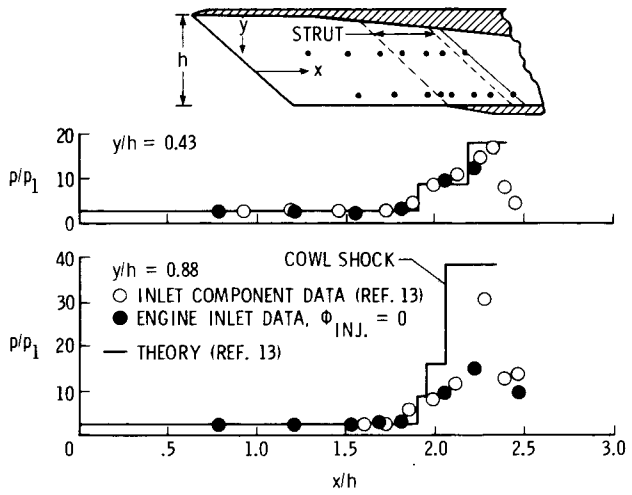

Fig. 10 Verification of inlet starting at inlet Mach number 6.

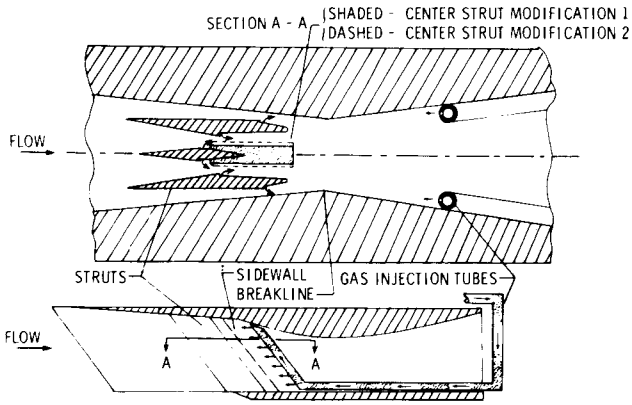

Fig. 11 Scramjet model with gas injection tubes.

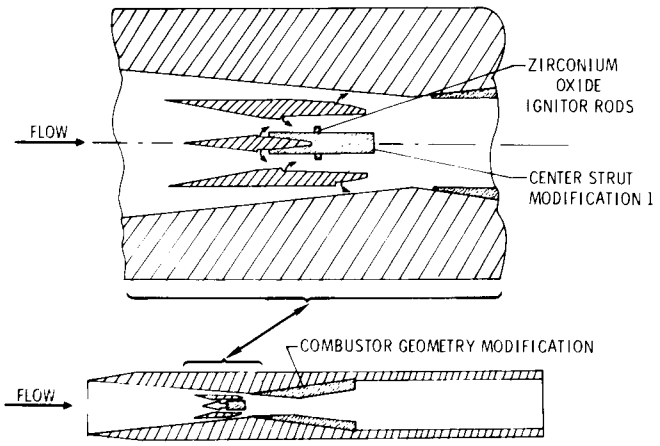

Fig. 12 Ignitor rods and geometry modifications.

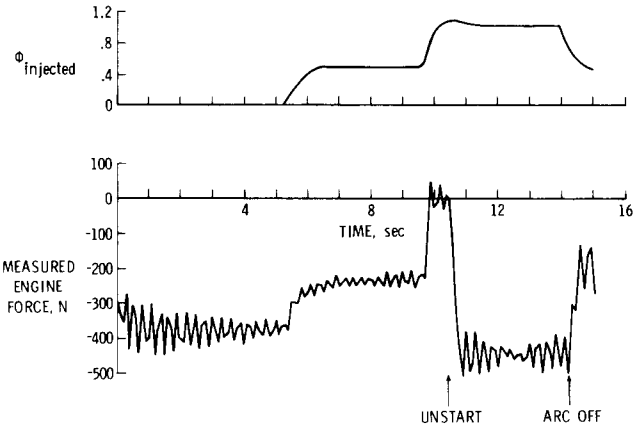

Fig. 13 Engine force variation with fuel injection at Mach 7 (no boundary layer ingestion).

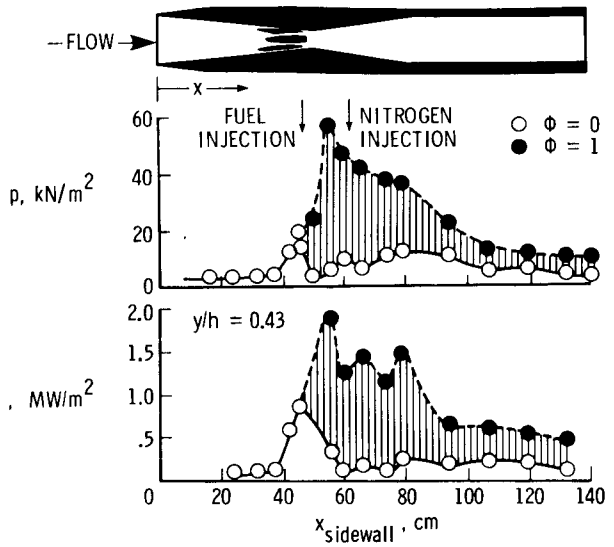

Fig. 14 Sidewall pressure and heating rate distributions at simulated Mach 7 flight conditions.

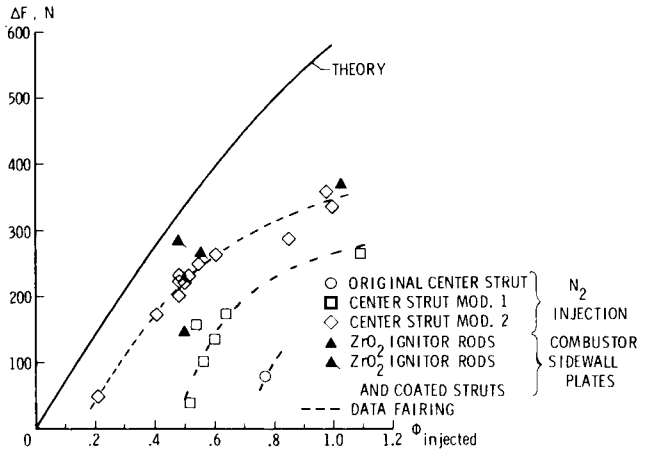

Fig. 15 Scramjet performance at Mach 7 as a function of injected fuel equivalence ratio.

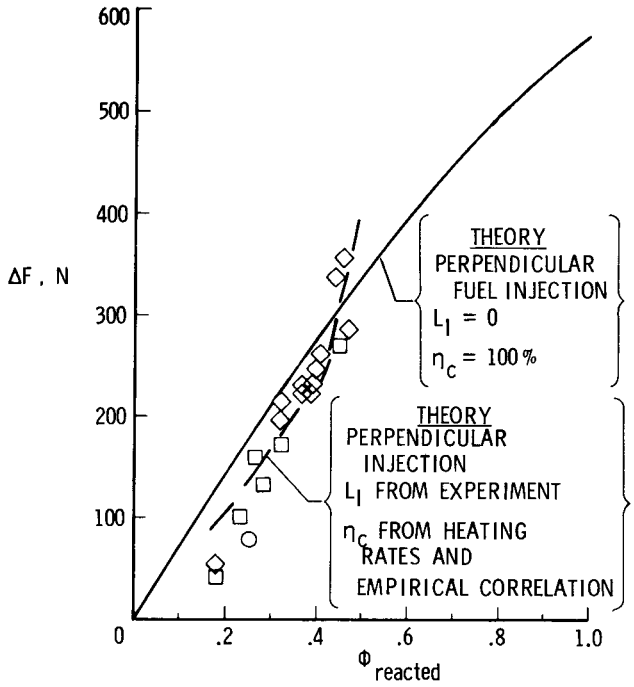

Fig. 16 Scramjet performance at Mach 7 as a function of reacted fuel equivalence ratio.

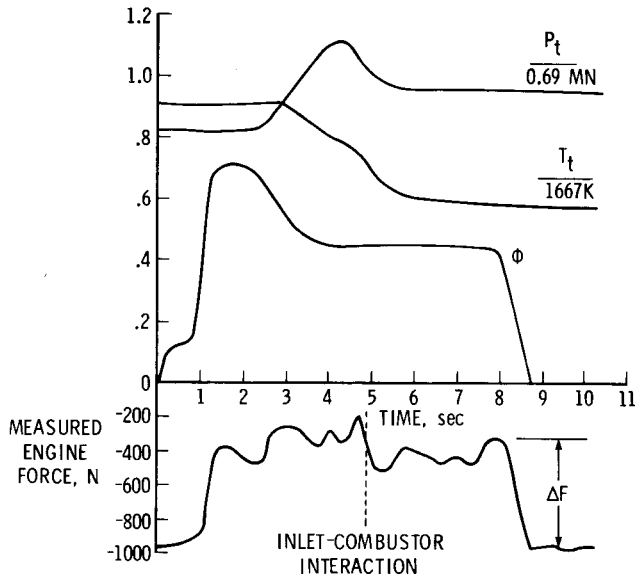

Fig. 18 Mach 4 test sequence and measured engine force.

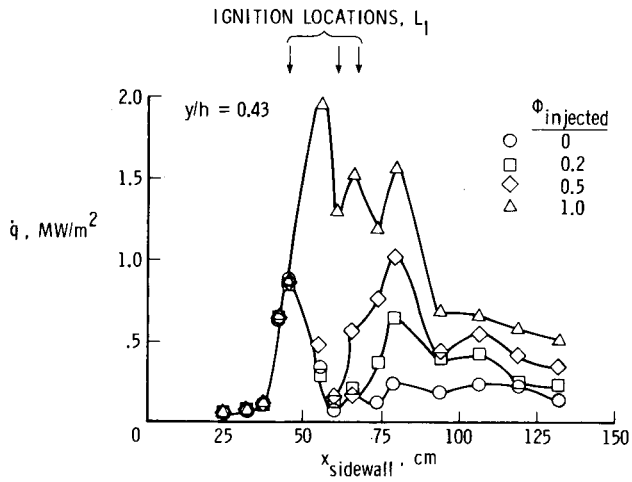

Fig. 17 Effect of fuel equivalence ratio on ignition location.

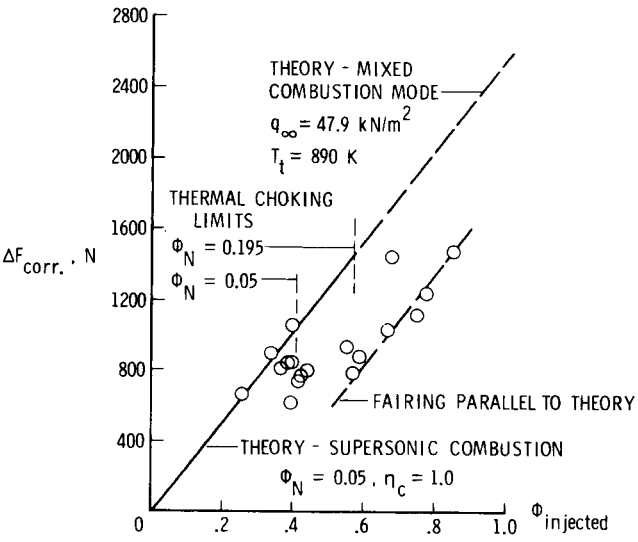

Fig. 19 Scramjet performance at Mach 4 as a function of injected fuel equivalence ratio

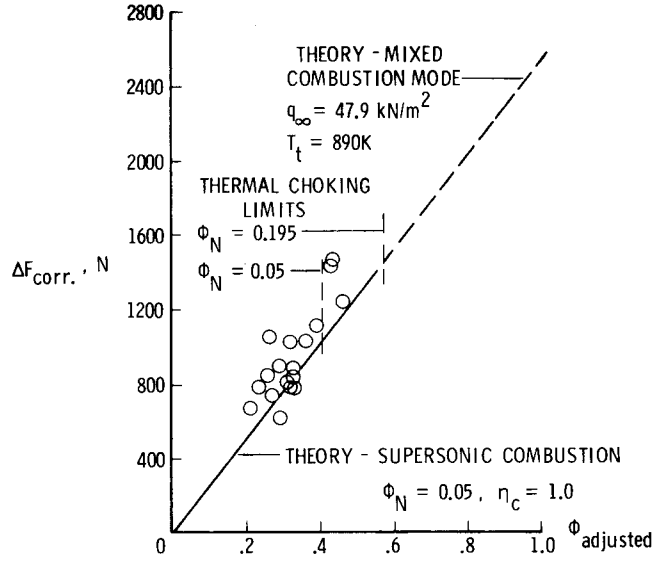

Fig. 20 Scramjet performance at Mach 4 as a function of adjusted fuel equivalence ratio.

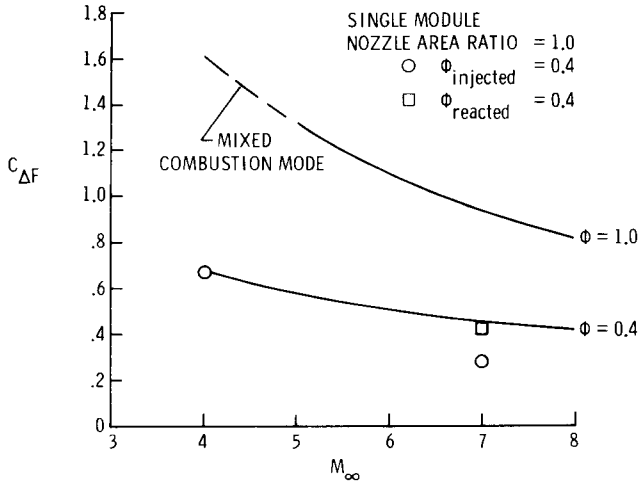

Fig. 21 Comparison of data with theory for ground tests.

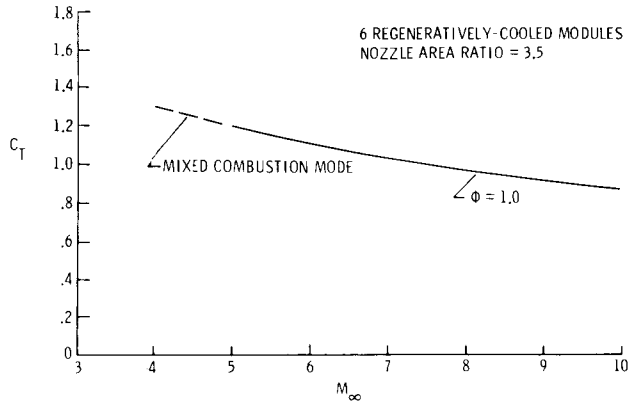

Fig. 22 Scramjet net installed flight performance.